Submitted to the Astrophysical Journal
Preprint typeset using LaTeX style emulateapj v. 2/19/04

arXiv:astro-ph/0703181v2 24 Aug 2007

PULSED X-RAY EMISSION FROM PULSAR A IN THE DOUBLE PULSAR SYSTEM J0737−3039

S. Chatterjee[1,2], B. M. Gaensler[1,2], A. Melatos[3], W. F. Brisken[4], B. W. Stappers[5,6]

Submitted to the Astrophysical Journal

ABSTRACT

The double pulsar system J0737−3039 is not only a test bed for General Relativity and theories of gravity, but also provides a unique laboratory for probing the relativistic winds of neutron stars. Recent X-ray observations have revealed a point source at the position of the J0737−3039 system, but have failed to detect pulsations or orbital modulation. Here we report on *Chandra X-ray Observatory* High Resolution Camera observations of the double pulsar. We detect deeply modulated, double-peaked X-ray pulses at the period of PSR J0737−3039A, similar in appearance to the observed radio pulses. The pulsed fraction is $\sim 70\%$. Purely non-thermal emission from pulsar A plausibly accounts for our observations. However, the X-ray pulse morphology of A, in combination with previously reported spectral properties of the X-ray emission, allows the existence of both non-thermal magnetospheric emission and a broad sinusoidal thermal emission component from the neutron star surface. No pulsations are detected from pulsar B, and there is no evidence for orbital modulation or extended nebular structure. The absence of orbital modulation is consistent with theoretical expectations of a Poynting-dominated relativistic wind at the termination shock between the magnetosphere of B and the wind from A, and with the small fraction of the energy outflow from A intercepted by the termination shock.

Subject headings: stars: neutron — pulsars: individual (J0737−3039A, J0737−3039B) — X-rays: stars

1. BACKGROUND

Binary neutron star systems are rare, and even among them, the double pulsar system J0737−3039 is extraordinary, since both the neutron stars are detected as radio pulsars. The system consists of the recycled 22.7 ms pulsar “A” (Burgay et al. 2003) and the young 2.8 s pulsar “B” (Lyne et al. 2004), in a 2.454 hr eccentric ($e = 0.09$) binary orbit which happens to be nearly edge-on to us. As well as being a test bed for General Relativity and theories of gravity (e.g. Kramer et al. 2006), the double pulsar is rich in observational phenomena, including a short eclipse of A by the magnetosphere of B and orbital modulation of the radio flux of B due to the influence of A (Lyne et al. 2004). The individual pulses from B show drifting features due to the impact of the low-frequency electromagnetic wave in the relativistic wind from A (McLaughlin et al. 2004b), while the eclipse of A is modulated at half the rotational period of B (McLaughlin et al. 2004c). Clearly, the two neutron stars have both gravitational and electromagnetic interactions with each other, and the double pulsar system should provide a unique laboratory to investigate the interactions between the magnetospheres and relativistic winds of the two pulsars.

In this context, the detection of X-ray emission from the J0737−3039 system (McLaughlin et al. 2004a; Pellizzoni et al. 2004; Campana et al. 2004) is particularly exciting. Energetic pulsars generate several forms of X-ray emission: quasi-blackbody emission from the cooling neutron star surface and/or from heated polar caps; pulsed non-thermal emission from the pulsar magnetosphere; and at larger distances from the pulsar, synchrotron emission from a pulsar wind nebula (PWN) powered by the relativistic particle outflow. All of these processes may be taking place in the J0737−3039 system (see, e.g., Kargaltsev et al. 2006). Specifically, the X-rays could be pulsed magnetospheric or thermal emission from pulsar A (as seen for several other recycled pulsars; see Zavlin 2006), could originate in the colliding winds of A and B (Lyutikov 2004), or could be produced by the shock generated when one or both of the pulsar winds interacts with the interstellar medium (Lyutikov 2004; Granot & Mészáros 2004).

The electrodynamics of pulsar winds have been studied in considerable detail through the extended PWNe typically seen around young and/or high-velocity pulsars (Gaensler & Slane 2006). In systems such as the Crab Nebula, the PWN is an expanding synchrotron bubble centered on the pulsar. Such nebulae act as calorimeters, revealing the geometry and energetics of the pressure-confined outflow and its termination shock. However, the termination shocks seen in such PWNe are typically at distances $\sim 10^6 - 10^9 R_{LC}$ from their pulsars (where the light cylinder radius of a pulsar rotating at a frequency f is $R_{LC} \equiv c/2\pi f$). In contrast, the two neutron stars in the double pulsar system are separated by $\lesssim 10^3 R_{LC,A}$ and only $6.6 R_{LC,B}$; a termination shock between them can thus probe the properties of a pulsar's relativistic wind at smaller separations from the central engine than ever studied before. Additionally, detection of an orbital phase dependence in the X-ray emission might be expected (e.g., Arons & Tavani 1993). Such variability could constrain the geometry of the emission site, thus

---

[1] School of Physics A29, The University of Sydney, NSW 2006, Australia; schatterjee, bgaensler@usyd.edu.au

[2] Harvard-Smithsonian Center for Astrophysics, 60 Garden Street, Cambridge, MA 02138

[3] School of Physics, University of Melbourne, Parkville VIC 3010, Australia; amelatos@physics.unimelb.edu.au

[4] National Radio Astronomy Observatory, P.O. Box O, Socorro, NM 87801; wbrisken@aoc.nrao.edu

[5] Stichting ASTRON, Postbus 2, 7990 AA Dwingeloo, The Netherlands; stappers@astron.nl

[6] Astronomical Institute “Anton Pannekoek”, University of Amsterdam, Kruislaan 403, 1098 SJ Amsterdam, The Netherlands

providing new insights into the wind physics close to the pulsar.

Here we report on *Chandra* observations of the double pulsar which have high enough time resolution to test for pulsations from either pulsar and for orbital variability, the latter of which might be expected in the bow shock or colliding winds interpretation. Forming histograms of count rates as a function of phase, we test for modulated X-ray emission at the periods of pulsar A and pulsar B, as well as for orbital modulation.

2. OBSERVATIONS AND DATA ANALYSIS

The J0737−3039 system was observed with the *Chandra X-ray Observatory* using the High Resolution Camera (HRC-S) in "timing mode", which provides the highest available time resolution, with events corrected for the instrumental wiring error and time-tagged to 16 μs accuracy. The observations spanned 10.5 binary orbits but were split into two segments for spacecraft operational reasons. The first segment of 55 ks began on 2006 February 28, while the second segment began $\sim$ 67 ks after the end of the first, and spanned 38 ks. The pulsar system was unambiguously detected as a point source in both segments, at a position $07^{\rm h}37^{\rm m}51\overset{\rm s}{.}22$ $-30°39'40\overset{''}{.}3$ (J2000), consistent with positions previously determined at X-ray and radio wavelengths (McLaughlin et al. 2004a; Chatterjee et al. 2005; Kramer et al. 2006) at the $\sim 0\overset{''}{.}5$ pointing accuracy of Chandra.

X-ray photons were extracted from a $1''$ radius circle at the detected position of the J0737−3039 system, and the times of arrival for the photons were corrected to the solar system barycenter using the JPL planetary ephemeris DE405. Of the 411 photons extracted, we estimate that $\sim$ 16 counts were contributed by the X-ray background. Of course, we cannot identify which of the extracted photons came from the background, and nor can we assign photons to the individual pulsars. Instead, we use TEMPO[7] and timing solutions from Kramer et al. (2006) to calculate the binary orbital phase and the rotational phases of both pulsars A and B at which each photon was emitted. In keeping with our request that the observation be split (if necessary) into integer orbit blocks, the orbital phase of the extracted photons ranged from 0.840 to 6.854 in the first segment, and from 0.497 to 4.531 in the second. Thus only $\sim$5% of the orbit was sampled 11 times, while the rest was uniformly sampled 10 times. In the analysis reported below, we have ignored the minor oversampling, but we have verified that discarding 3 detected photons to force uniformity in orbital coverage does not affect our results.

3. PULSATIONS FROM PSR J0737−3039A

Forming a histogram of count rate as a function of the rotational phase of A, we detect X-ray pulses from pulsar A, as illustrated in Figure 1. The uncertainties on each bin (here and elsewhere in this work) are 1σ (68%) confidence intervals estimated according to Gehrels (1986). The pulsations are double-peaked and deeply modulated, with a pulsed fraction $f \equiv (\mathrm{Max} - \mathrm{Min})/(\mathrm{Max} + \mathrm{Min})$ of $0.74^{+0.18}_{-0.14}$. To estimate the significance of the detection, we calculate the Pearson χ^2 statistic for the pulse profile with 16 bins (degrees of freedom ν=15), and find $\chi^2/\nu = 7.05$, corresponding to a probability of only 10^{-15} ($\sim 8\sigma$) that the profile is drawn from a uniform distribution.

A visual comparison of the radio pulse profile of PSR J0737−3039A (Manchester et al. 2005) with the X-ray profile shows a distinct resemblance (Figure 1). Demorest et al. (2004) model the radio pulse as two cuts through a wide cone of emission centered on a single magnetic pole of A, which has its spin and magnetic axes nearly aligned ($4° \pm 3°$). Although a wide range of misalignment is currently permitted by radio observations (Manchester et al. 2005), both peaks of the observed pulse appear to come from one magnetic pole, implying a very wide fan beam in some geometries. The X-ray pulse profile also shows two peaks, whose locations fall within the range in pulse phase delimited by the radio peaks when the pulses are phase-aligned.[8] This suggests that the X-ray emission is from a narrower cone than the radio beam. Specifically, the peaks in the X-ray profile (Figure 1) are located at pulse phases $\phi_A \sim 0.27$ and ~ 0.77, as estimated by binning the observed X-ray photons at various resolutions, and the peak-to-peak separation is $\sim 0.50 \pm 0.01$ ($182° \pm 3°$), while the peaks in the 1.4 GHz radio profile (Manchester et al. 2005) are at $\phi_A = 0.234$ and $\phi_A = 0.789$, separated by $\sim 200°$, and the outer rims of the radio emission profile are at $\phi_A = 0.164, 0.836$. The X-ray emission also shows a significant "bridge" between the two peaks, implying that the cone of X-ray emission is (partially) center-filled in this model, unlike the broader, hollow radio emission cone.

The detected pulses are quite unlike the typical X-ray emission observed from other recycled pulsars with comparable spin parameters (e.g., PSR J0437−4715, Zavlin et al. 2002; Bogdanov et al. 2006; Zavlin 2006), which show broad, roughly sinusoidal pulsations with low pulsed fractions and thermal spectra. Instead, the pulsations from pulsar A resemble non-thermal pulses seen only from the most energetic recycled pulsars (e.g., PSR B1821−24, Rutledge et al. 2004), even though A is slower rotating and has a lower spindown energy loss rate ($\dot{E}_A = 5.9 \times 10^{33}$ erg s^{-1}). In this context, we note that the formation scenario for double neutron star binary systems (Stairs 2004) can result in a shorter accretion episode and thus a higher surface magnetic field strength compared to other recycled pulsars. Pulsar A has an inferred dipole magnetic field $B_A = 6.4 \times 10^9$ G, comparable to PSR B1821−24 and the binary pulsar B1534+12, but significantly higher than other recycled pulsars that show predominantly thermal X-ray emission. Both pulsars B1821−24 and J0737−3039A also lie above the death line for curvature radiation estimated by Harding et al. (2005), suggesting that the processes that power non-thermal magnetospheric emission in PSR B1821−24 may also operate for pulsar A, although the two differ substantially in period and $\dot{E}$.

The absence of any useful energy resolution in *Chandra*

---

[7] http://www.atnf.csiro.au/research/pulsar/timing/tempo

[8] Rutledge et al. (2004) show that absolute phase alignment is possible at the 60 μs level between HRC-S and radio observations of the recycled pulsar PSR B1821−24. Since we have to predict and account for both orbital and rotational phase, our timing errors are somewhat larger, but insignificant compared to the bin width of $\sim$1.4 ms.

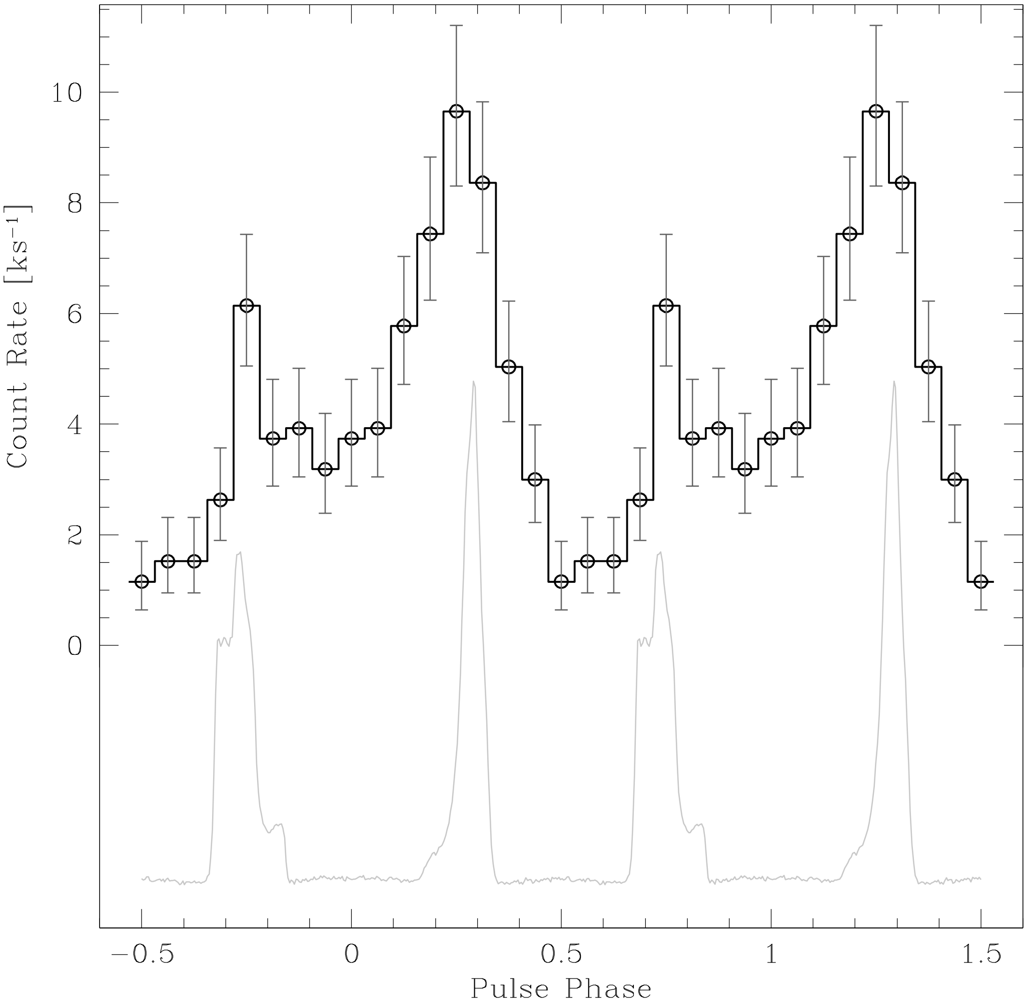

FIG. 1.— X-ray pulse profile of pulsar A, obtained by folding 89 ks of *Chandra* HRC-S data with TEMPO and a DE405 timing solution. The uncertainties on each bin (here and elsewhere in this work) are 1σ (68%) confidence intervals estimated according to Gehrels (1986). The pulse profile is shown twice for clarity, and a radio pulse profile obtained at 1.4 GHz (Manchester et al. 2005) is plotted below (in arbitrary units) for comparison. Both profiles are folded using the radio timing solution, and are therefore aligned in phase.

HRC data precludes spectral fits to the data, but previous *Chandra* ACIS observations can be well-modeled by a power law with a photon index $\Gamma \sim 2.9 \pm 0.4$ (McLaughlin et al. 2004a), and *XMM* data is well-fit by a power law with a photon index $\Gamma \sim 3.5^{+0.5}_{-0.3}$ (Pellizzoni et al. 2004). Joint fits to the *Chandra* and *XMM* data (Campana et al. 2004) allow for both power law ($\Gamma = 4.2^{+2.1}_{-1.2}$) and thermal black body ($kT_{bb} = 0.20 \pm 0.02$ keV) interpretations. Similar fit parameters ($\Gamma \sim 3$ or $kT_{bb} \sim 0.2$ keV) were found by Kargaltsev et al. (2006) as well. Additionally, Campana et al. (2004) show that a two-component fit with a fixed power law index $\Gamma = 2$ and a black body component ($kT_{bb} = 0.16 \pm 0.04$ keV) is consistent with the *Chandra* ACIS and *XMM* data, although two components are not statistically required.

The X-ray spectrum, in combination with our detection of sharp, double-peaked X-ray pulses, is thus consistent with a purely magnetospheric origin for the X-ray emission, but it is also possible that the observed X-ray pulsations consist of both non-thermal magnetospheric emission and broad sinusoidal thermal pulsations from the hot polar cap. The pulse profile of A shows a floor of X-ray emission (Figure 1), corresponding to a count rate of $\approx 1.5 \pm 0.6$ cts ks^{-1} at every phase. An image of the off-pulse counts reveals no extended nebular structure, and their distribution is consistent with the on-pulse photons. Other recycled pulsars also show emission at all pulse phases, whether their pulsations are broad and thermal (e.g., PSR J0437−4715, Zavlin et al. 2002; Bogdanov et al. 2006; Zavlin 2006) or narrower and primarily non-thermal (e.g., PSR J0218+4232, Kuiper et al. 2002; PSR B1821−24, Rutledge et al. 2004). Such unpulsed emission is usually ascribed to thermal X-rays emitted from the neutron star surface. Assuming that the entire X-ray flux of the double pulsar system arises only from the combined thermal and non-thermal emission from PSR J0737−3039A, we find that the maximum amplitude sinusoid $A(1 + \sin 2\pi(\phi - \phi_0))$ that is consistent with the observed profile at 1σ could account for as much as $\sim 60\%$ of the observed X-ray counts, although the actual fraction is likely to be far lower. Rotational phase-resolved spectroscopy with substantially more X-ray counts will be required to verify or rule out such a two-component model.

In order to investigate possible orbital variations in the X-ray pulse profile of A, 9-bin pulse profiles were constructed for each quadrant of the orbit. Each of the four profiles was then compared to the pulse profile constructed by averaging the other three quadrants. The resulting χ^2/ν values range between 0.8 and 1.3 (with $\nu = 9$ degrees of freedom), consistent with no variations. While we lack the S/N to definitively rule out any differences between the X-ray pulse profiles, no orbital variations are detected in the radio pulse profiles of A either (e.g. Kramer et al. 2006).

We note in passing that our estimate of the pulsed fraction $f = 0.74^{+0.18}_{-0.14}$ is only marginally consistent with the upper limit of 60% on the pulsed fraction (assuming sinusoidal pulses) inferred by Pellizzoni et al. (2004) from *XMM-Newton* observations. Since the detected pulse is non-sinusoidal, a direct comparison is not possible, but $\sim 60\%$ of our detected photons are above the estimated minimum count rate baseline, and $\gtrsim 51\%$ are $> 1\ \sigma$ above the baseline level. The *XMM* pn observations of Pellizzoni et al. (2004), which were in continuous clocking mode, were totally dominated by the background due to the one-dimensional readout, while the *XMM* MOS chips lack the time resolution to detect pulses from A, leading to a limit which is less robust compared to the *Chandra* HRC detection presented here.

4. NON-DETECTION OF PSR J0737−3039B

We repeated the analysis described in § 3 for PSR J0737−3039B. The results are shown in Figure 2. No X-ray pulsations are detected, either by folding the full span of data, or by selecting counts which are in the lowest emission bins of the pulse profile of A, $0.46875 < \phi_A < 0.65625$. For the folded profile from the entire data span, we calculate $\chi^2/\nu = 1.34$, corresponding to a 17% probability that the data are drawn from a uniform distribution. As described by Leahy et al. (1983), epoch folding is not as sensitive to broad, smooth pulses as the family of Rayleigh statistics Z^2_m, which also avoid the need to bin data. Therefore, we also calculated the H statistic ($H \equiv \mathrm{Max}(Z^2_m - 4m + 4)$, for $1 \leq m \leq 20$; de Jager et al. 1989), which is well suited to searching for an unknown modulation shape. We find $H = 0.035$, at $m = 1$, corresponding to a null hypothesis probability (i.e., the probability that we are sampling a uniform distribution) close to unity.

Pulsar B shows significant enhancements in radio emission at some parts of its orbit (Lyne et al. 2004), but folding X-ray photons selected from those orbital phase ranges does not show any evidence for pulsations either. The non-detection is unsurprising, since pulsar B has rotational parameters and a spindown energy loss rate ($\dot{E}_B = 1.7 \times 10^{30}$ erg s^{-1}) similar to other "ordinary" pulsars (ages $\sim 10^6 - 10^8$ yr), which are not known for their X-ray emission. The spindown luminosity of pulsar B is only $\sim 3 \times 10^{-4}\ \dot{E}_A$, and so pulsar A is expected to dominate any X-ray emission from the system.

5. LIMITS ON ORBITAL MODULATION

Systems such as the Crab nebula (Kennel & Coroniti 1984; Gallant & Arons 1994) and the nebula around PSR B1509−58 (Gaensler et al. 2002) provide the best current constraints on the behavior of pulsar winds at large distances ($\sim\ 10^6 - 10^9 R_{LC}$) from the neutron star, but few constraints exist for the close-in behavior. The magnetization parameter σ, the ratio of Poynting flux to the kinetic energy flux in the wind, is a key descriptor of such systems. Optical, near-infrared, and X-ray images at sub-arcsecond resolution reveal that the shock has an axisymmetric structure of equatorial arcs (wisps) and polar jets (knots) that vary on short time-scales (Hester et al. 2002; Pavlov et al. 2003; Melatos et al. 2005), and that the wind transforms from a Poynting-dominated outflow ($\sigma \gg 1$) near the pulsar to a kinetic-energy-dominated outflow ($\sigma < 1$) at the termination shock (Kennel & Coroniti 1984). Recent work has begun to elucidate the collimation mechanism that produces the axisymmetric structure (e.g., Komissarov & Lyubarsky 2004), while the conversion of Poynting flux to mechanical energy remains poorly understood.

The wind interaction of a neutron star with a stellar binary companion allows constraints on the wind behavior at $\sim 10^4 R_{LC}$, and such interaction can produce radio and high energy emission signatures. For example, the Be star—pulsar binary B1259−63 produces unpulsed radio emission (Ball et al. 1999) as well as unpulsed high energy emission (e.g., Grove et al. 1995), which arise from the shock formed between the stellar outflow and the pulsar wind (Tavani & Arons 1997). The interaction of the pulsar B1957+20 with its white dwarf binary companion is expected to produce orbital modulation in the X-ray emission (see, e.g., Arons & Tavani 1993; Michel 1994), although the observational evidence for such modulation (Stappers et al. 2003; Huang & Becker 2007) is not significant.

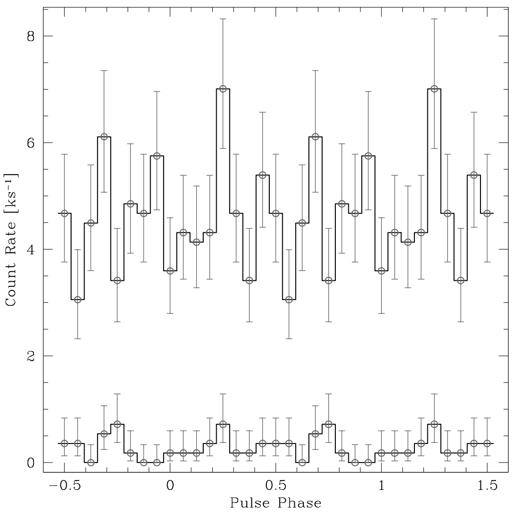

Fig. 2.— Non-detection of pulsations from PSR J0737−3039B. 89 ks of *Chandra* HRC-S data were folded at the rotational phase of B, as predicted by Tempo, but no pulsations were detected. Two pulse periods are shown for clarity. Further, we extracted 26 photons detected in the off-pulse phase range of A, $0.46875 < \phi_A < 0.65625$, corresponding to the three bins with lowest photon counts in Figure 1. The folded counts are shown on the same scale (the lower pulse profile in the figure). Again, no significant pulsations were detected.

As opposed to the interaction between a neutron star relativistic wind and the particle wind of a stellar companion, the double pulsar presents a situation where the relativistic wind interacts with the magnetosphere of another neutron star. Additionally, the system separation is $\lesssim 10^3 R_{LC,A}$ and only $6.6 R_{LC,B}$. The detection of orbital modulation in the system would thus be of particular interest, since it probes the behavior of the pulsar wind in a high-σ regime. We note that Kargaltsev et al. (2006) find possible orbital phase dependence for the double neutron star binary B1534+12, but not for the J0737−3039 system. Their result is based on earlier *XMM* and *Chandra* ACIS data that lacked the time resolution to detect pulsations from pulsar A.

Given our detection of deeply modulated pulsed emission from PSR J0737−3039A, we attempted to detect orbital modulation in the X-ray emission by folding X-ray photons from the off-pulse phase of A, $0.46875 < \phi_A < 0.65625$, corresponding to the three bins with lowest photon counts in Figure 1. The 25 counts thus selected from the observation (corresponding to a reduced effective exposure of 16.7 ks) were folded as a function of orbital phase, and the results are shown in the top panel of Figure 3. We find an apparent enhancement at a phase ∼0.69. At the epoch of observation, that phase bin includes an orbital longitude $\omega = 0°$, corresponding to A's crossing of the ascending node of the orbit. However, there is no obvious physical mechanism that could produce such an enhancement, and the binned distribution has $\chi^2/\nu = 1.45$, corresponding to a chance probability of 11.5%. As in §4, we calculate the H statistic with the un-binned orbital phase values. We find $H = 7.35$ at the fifth harmonic Z_5^2, which allows the null hypothesis that we have sampled uniformly distributed data at $\sim 5\%$, a probability that is small but not insignificant.

We also check for the enhancement by folding all the X-ray photons, and by selecting and folding photons from the bridge of emission between the two peaks of A's pulse profile ($-0.15625 < \phi_A < 0.03125$), where the contribution of the pulsar itself is reduced. The results are shown in the middle and bottom panels of Figure 3, and in each case, we again calculate the H statistic. $H = 1.66$ at $m = 1$ when including all the extracted photons, corresponding to a null hypothesis probability of 52%. For the photons chosen from between the two peaks of A's pulse, $H = 0.023$ at $m = 1$, which allows the null hypothesis at a probability close to unity. Together, these results lend weight to the conclusion that the apparent orbital modulation seen above (with a chance probability of 5%) is, in fact, not real. We have also confirmed the absence of significant modulation by binning as a function of orbital longitude rather than phase, with very similar results. As outlined in § 3, it is more likely that the unpulsed X-rays have their origin in thermal emission from the surface of pulsar A. We thus confirm the negative result found by Kargaltsev et al. (2006).

From the drifting sub-pulses detected in B's radio emission (McLaughlin et al. 2004b), it is apparent that the low-frequency electromagnetic wave in the relativistic wind from A influences the emission of pulsar B, and several models have been proposed where the formation of a shock between the two pulsars should produce orbital modulation in their emission (e.g. Lyutikov 2004; Granot & Mészáros 2004; Turolla & Treves 2004).

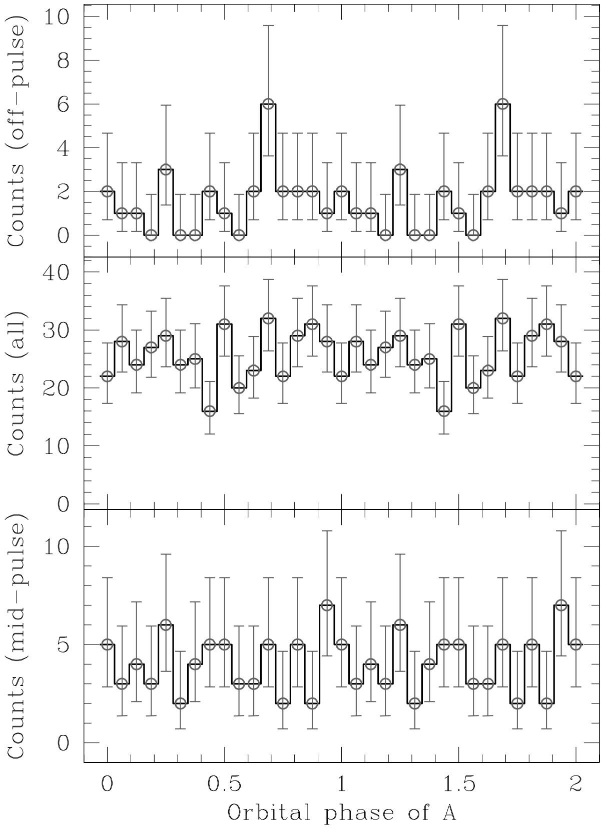

FIG. 3.— Searching for orbital modulation in X-ray emission from the J0737−3039 system. In all cases, the orbit is plotted twice for clarity. *Top:* We extract 25 photons detected in the off-pulse phase range of A, $0.46875 < \phi_A < 0.65625$, corresponding to the three bins with lowest photon counts in Figure 1. Folding at the binary phase shows an enhancement at an orbital phase ∼0.69. At the epoch of observation, that phase bin encompasses an orbital longitude $\omega = 0°$, when A crosses the ascending node of the orbit. *Middle:* Folding all detected photons at the binary phase does not show such an enhancement. Note that we lack enough counts to detect or constrain the eclipse of A at an orbital longitude $\omega = 90°$. *Bottom:* We extract 65 photons in the mid-pulse of A, $-0.15625 < \phi_A < 0.03125$, corresponding to the three bins between the peaks of the profile in Figure 1. The absence of any significant enhancement confirms that the apparent signal in the top panel is spurious.

However, only a small fraction of the wind power emitted by A (and half of the power emitted by B) is intercepted by the shock between the two pulsars, reducing proportionately the maximum X-ray flux that the shock emits. For example, if we assume that the wind energy is radiated isotropically from A, and that it is intercepted by a sphere centered on B with radius $R_{LC,B}$, then the power intercepted by the shock, $\dot{E}_s = 0.006\dot{E}_A + 0.5\dot{E}_B \approx 0.006\dot{E}_A$. If, instead, A's wind is intercepted at the surface where pressure balance is achieved between the wind from A and the magnetosphere of B, at $\sim$ 0.20 lt-s from B (Lyne et al. 2004), then we have $\dot{E}_s = 0.001\dot{E}_A + 0.5\dot{E}_B \approx 0.001\dot{E}_A$. Finally, if the shock roughly coincides with the region centered on B that eclipses the radio pulses from A, we have $\dot{E}_s = 10^{-5}\dot{E}_A + 0.5\dot{E}_B \approx 1.5 \times 10^{-4}\dot{E}_A$ (although the processes that contribute to radio eclipses are likely to be quite different from those that cause X-ray emission).

Of course, the wind radiated from A is unlikely to be isotropic, especially if the magnetic and rotational axes are nearly-aligned (Demorest et al. 2004), and the shock geometry is not described simply by intersecting spheres centered on A and B. Nevertheless, the conservative geometric estimates above demonstrate that the X-ray power output from the shock is $\dot{E}_s \lesssim 0.006\dot{E}_A$, possibly modulated at the orbital period. Interestingly, spectral fits to the *Chandra* and *XMM* data imply an X-ray efficiency $L_x/\dot{E}_A \lesssim 2\times10^{-4}$ (Campana et al. 2004), where L_x is the X-ray luminosity in the 0.5—10 keV range. Thus, if the entire $\dot{E}_s$ were converted to X-ray emission, at least two of our proposed scenarios above would have resulted in a higher X-ray efficiency for the J0737−3039 system than actually observed. Since we detect X-ray pulses from A which account for a significant proportion (and arguably ∼100%) of the observed X-ray emission, all of $\dot{E}_s$ evidently does not appear as X-ray emission. (We note that for $\dot{E}_A = 5.9\times10^{33}$ erg s^{-1}, the relations derived by Possenti et al. (2002) for X-ray luminosity in the 2—10 keV range predict a maximum X-ray efficiency $L_x/\dot{E}_A < 0.005$, consistent with observations.)

The wind interaction in the double pulsar system is fundamentally different energetically from wind confinement in a Crab-like pulsar wind nebula, since the termination shock of the wind is much closer to pulsar A ($\lesssim 10^3 R_{LC,A}$) than in Crab-like nebulae ($\sim 10^8 R_{LC}$). All modern wind models, whether for a steady-state, force-free, magnetohydrodynamic outflow (Contopoulos & Kazanas 2002) or a wave-like, striped outflow (Melatos & Melrose 1996; Lyubarsky & Kirk 2001), predict values of the magnetization parameter $\sigma \gg 1$ (probably $\gtrsim 100$) at these distances, unlike termination shocks in pulsar wind nebulae, where $\sigma \ll 1$. For a high-σ shock, Kennel & Coroniti (1984) estimate an upper limit on the power fed into the accelerated electrons (and hence on the X-ray luminosity of the shock) of $\dot{E}_s/(8\sqrt{\sigma})$. In summary, as a result of the high expected value of σ and the small solid angle over which the wind from A is intercepted by B, the shock produced at the interaction region is unlikely to show significant X-ray emission. Similar arguments apply to the absence of unpulsed radio emission from the system (Chatterjee et al. 2005) as well.

6. CONCLUSIONS

With 89 ks of *Chandra* HRC observations, we have detected deeply modulated emission from PSR J0737−3039A. The off-pulse emission reveals no extended structure. No pulsations were detected from PSR J0737−3039B, and no orbital modulation was detected either. Although we cannot absolutely rule out orbital modulation or emission from other mechanisms such as bow shocks, we have shown that the entire X-ray emission from the J0737−3039 system can be explained as arising from pulsar A alone, either as non-thermal magnetospheric emission, or as a combination of magnetospheric and thermal emission. Pulse phase-resolved spectroscopy will allow discrimination between these two scenarios.

Like the dog that did not bark in the night, the absence of significant and detectable orbital modulation in the X-ray emission from the J0737−3039 system is noteworthy. The wind from pulsar A impinges on and compresses the magnetosphere of B, leading to deep orbital modulation in the detected radio pulsations from B (Lyne et al. 2004), and the impact of the low-frequency electromagnetic wave in the relativistic wind from A is also seen in the drifting sub-pulses of emission observed from B (McLaughlin et al. 2004b). Given the strong influence of A on the radio emission from B, it may seem natural to ascribe the X-ray emission from the PSR J0737−3039 system to a particle shock formed at the wind-magnetosphere interaction site. As we show here, such an interpretation is neither favored by theory, nor required by the X-ray observations. Our observations reveal no significant orbitally modulated shock emission, consistent with models for relativistic winds that require a Poynting-dominated wind close to the pulsar, and with only a small fraction of the energy outflow from A interacting with the termination shock.

We thank Michael Kramer for making current timing solutions available for PSR J0737−3039A and B, Dick Manchester for providing us radio pulse profiles, Scott Ransom for creating PRESTO, and for his guidance in using it, and Zaven Arzoumanian for helpful discussions about TEMPO. We also thank George Pavlov, Slavko Bogdanov, Nanda Rea, and the anonymous referee for their helpful comments on the manuscript. SC acknowledges support from the University of Sydney Postdoctoral Fellowship program. Support for this work was provided by NASA through Chandra award GO5-6046X to the Harvard College Observatory.

REFERENCES

Arons, J., & Tavani, M. 1993, ApJ, 403, 249

Ball, L., Melatos, A., Johnston, S., & Skjæ Raasen, O. 1999, ApJ, 514, L39

Bogdanov, S., Grindlay, J. E., & Rybicki, G. B. 2006, ApJ, 648, L55

Burgay, M., D'Amico, N., Possenti, A., Manchester, R. N., Lyne, A. G., Joshi, B. C., McLaughlin, M. A., Kramer, M., Sarkissian, J. M., Camilo, F., Kalogera, V., Kim, C., & Lorimer, D. R. 2003, Nature, 426, 531

Campana, S., Possenti, A., & Burgay, M. 2004, ApJ, 613, L53

Chatterjee, S., Goss, W. M., & Brisken, W. F. 2005, ApJ, 634, L101

Contopoulos, I., & Kazanas, D. 2002, ApJ, 566, 336

de Jager, O. C., Swanepoel, J. W. H., & Raubenheimer, B. C. 1989, A&A, 221, 180

Demorest, P., Ramachandran, R., Backer, D. C., Ransom, S. M., Kaspi, V., Arons, J., & Spitkovsky, A. 2004, ApJ, 615, L137

Gaensler, B. M., Arons, J., Kaspi, V. M., Pivovaroff, M. J., Kawai, N., & Tamura, K. 2002, ApJ, 569, 878

Gaensler, B. M., & Slane, P. O. 2006, ARA&A, 44, 17

Gallant, Y. A., & Arons, J. 1994, ApJ, 435, 230

Gehrels, N. 1986, ApJ, 303, 336

Granot, J., & Mészáros, P. 2004, ApJ, 609, L17

Grove, J. E., Tavani, M., Purcell, W. R., Johnson, W. N., Kurfess, J. D., Strickman, M. S., & Arons, J. 1995, ApJ, 447, L113+

Harding, A. K., Usov, V. V., & Muslimov, A. G. 2005, ApJ, 622, 531

Hester, J. J., Mori, K., Burrows, D., Gallagher, J. S., Graham, J. R., Halverson, M., Kader, A., Michel, F. C., & Scowen, P. 2002, ApJ, 577, L49

Huang, H. H., & Becker, W. 2007, A&A, 463, L5

Kargaltsev, O., Pavlov, G. G., & Garmire, G. P. 2006, ApJ, 646, 1139

Kennel, C. F., & Coroniti, F. V. 1984, ApJ, 283, 694

Komissarov, S. S., & Lyubarsky, Y. E. 2004, MNRAS, 349, 779

Kramer, M., Stairs, I. H., Manchester, R. N., McLaughlin, M. A., Lyne, A. G., Ferdman, R. D., Burgay, M., Lorimer, D. R., Possenti, A., D'Amico, N., Sarkissian, J. M., Hobbs, G. B., Reynolds, J. E., Freire, P. C. C., & Camilo, F. 2006, Science, 314, 97

Kuiper, L., Hermsen, W., Verbunt, F., Ord, S., Stairs, I., & Lyne, A. 2002, ApJ, 577, 917

Leahy, D. A., Elsner, R. F., & Weisskopf, M. C. 1983, ApJ, 272, 256

Lyne, A. G., Burgay, M., Kramer, M., Possenti, A., Manchester, R. N., Camilo, F., McLaughlin, M. A., Lorimer, D. R., D'Amico, N., Joshi, B. C., Reynolds, J., & Freire, P. C. C. 2004, Science, 303, 1153

Lyubarsky, Y., & Kirk, J. G. 2001, ApJ, 547, 437

Lyutikov, M. 2004, MNRAS, 353, 1095

Manchester, R. N., Kramer, M., Possenti, A., Lyne, A. G., Burgay, M., Stairs, I. H., Hotan, A. W., McLaughlin, M. A., Lorimer, D. R., Hobbs, G. B., Sarkissian, J. M., D'Amico, N., Camilo, F., Joshi, B. C., & Freire, P. C. C. 2005, ApJ, 621, L49

McLaughlin, M. A., Camilo, F., Burgay, M., D'Amico, N., Joshi, B. C., Kramer, M., Lorimer, D. R., Lyne, A. G., Manchester, R. N., & Possenti, A. 2004a, ApJ, 605, L41

McLaughlin, M. A., Kramer, M., Lyne, A. G., Lorimer, D. R., Stairs, I. H., Possenti, A., Manchester, R. N., Freire, P. C. C., Joshi, B. C., Burgay, M., Camilo, F., & D'Amico, N. 2004b, ApJ, 613, L57

McLaughlin, M. A., Lyne, A. G., Lorimer, D. R., Possenti, A., Manchester, R. N., Camilo, F., Stairs, I. H., Kramer, M., Burgay, M., D'Amico, N., Freire, P. C. C., Joshi, B. C., & Bhat, N. D. R. 2004c, ApJ, 616, L131

Melatos, A., & Melrose, D. B. 1996, MNRAS, 279, 1168

Melatos, A., Scheltus, D., Whiting, M. T., Eikenberry, S. S., Romani, R. W., Rigaut, F., Spitkovsky, A., Arons, J., & Payne, D. J. B. 2005, ApJ, 633, 931

Michel, F. C. 1994, ApJ, 431, 397

Pavlov, G. G., Teter, M. A., Kargaltsev, O., & Sanwal, D. 2003, ApJ, 591, 1157

Pellizzoni, A., De Luca, A., Mereghetti, S., Tiengo, A., Mattana, F., Caraveo, P., Tavani, M., & Bignami, G. F. 2004, ApJ, 612, L49

Possenti, A., Cerutti, R., Colpi, M., & Mereghetti, S. 2002, A&A, 387, 993

Rutledge, R. E., Fox, D. W., Kulkarni, S. R., Jacoby, B. A., Cognard, I., Backer, D. C., & Murray, S. S. 2004, ApJ, 613, 522

Stairs, I. H. 2004, Science, 304, 547

Stappers, B. W., Gaensler, B. M., Kaspi, V. M., van der Klis, M., & Lewin, W. H. G. 2003, Science, 299, 1372

Tavani, M., & Arons, J. 1997, ApJ, 477, 439

Turolla, R., & Treves, A. 2004, A&A, 426, L1

Zavlin, V. E. 2006, ApJ, 638, 951

Zavlin, V. E., Pavlov, G. G., Sanwal, D., Manchester, R. N., Trümper, J., Halpern, J. P., & Becker, W. 2002, ApJ, 569, 894